Quantitative Approach on Image Fusion Evaluation

ZHENGMAO YE[1], HUA CAO[2], SITHARAMA IYENGAR[2], HABIB MOHAMADIAN[1]
[1]Southern University, Baton Rouge, LA 70813, USA

[2]Louisiana State University, Baton Rouge, LA 70803, USA

Abstract: - Image registration and fusion are conducted using an automated approach, which applies automatic adaptation from frame to frame with the threshold parameters. Rather than qualitative approach, quantitative measures have been proposed to evaluate outcomes of image fusion. Concepts of the discrete entropy, discrete energy, mutual information and information redundancy have been introduced. Both Canny Edge Detector and control point identification are employed to extract retinal vasculature using the adaptive exploratory algorithms. The shape similarity criteria have been used for control point matching. The Mutual-Pixel-Count maximization based optimal procedure has also been developed to adjust the control points at the sub-pixel level. Then the global maxima equivalent result has been derived by calculating Mutual-Pixel-Count local maxima. Both cases of image fusion practices are satisfactory whose testing results are evaluated on a basis of information theories.

Key-Words: - Image Fusion, Image Registration, Histogram, Energy, Discrete Entropy, Information Redundancy

1 Introduction

Comparison between angiogram grayscale and fundus color images is generally required in order to identify dynamic aspects of circulation in practical applications and evaluate various retinal vascular disorders. Regular methods for medical image registration and fusion are either area-based or feature-based. Mutual Information is the frequently used optimization measurement in the area-based fusion. Maximization is the major approach of the area-based technique [1]. We employed the MI concept and simplified it to Mutual-Pixel-Count (MPC). The MPC measures the overlap pixels of the retinal vasculature. When images are perfectly geometrically aligned, the feature-based fusion method extracts and matches the common structures (features) from two images. It has been shown to receive higher successful rate at the multi-modality fusion scenario [1-5] than the area-based method. The feature refers to the salient structures, such as the central line of vessels and vessel bifurcation points in the retinal network. Depend on the transformation model, feature-based method requires a certain number of control points. The proposed approach selects a combined method, which uses the feature-based method in image registration and the area-based method in image fusion. For the feature-based registration, the adaptive exploratory algorithm has been used to identify the global direction change pixel at the Canny edges. By locating control points at the global direction change pixel, local direction changes can be efficiently avoided. For the area-based fusion, MPC is introduced, which is a new and unique concept in the biomedical image fusion area, especially for the fusion accuracy measurement. The fusion result is assumed to be optimal when MPC reaches the maximum value. From the information theory, concepts of discrete entropy, component energy and information redundancy are introduced to evaluate all the results of image fusion. In this case, both quantitative measures and qualitative observations are used together in this research [1-15].

2 Retinal Image Acquisition

Retinal images presented in this paper were taken by a Topcon TRC-50EX fundus camera. The subjects of the retinal images were five Cynomolgus monkeys of 4 to 4.5 years of age and 2.5 to 3 kg body weight with the normal eyes [3]. The experimental monkey was anesthetized with the intramuscular ketamine (7-10mg/kg), xylazine (0.6-1 mg/kg), and intravenous pentobarbital (25-30 mg/kg). Administration of the anesthetics was repeated alternately every 30 minutes as required to maintain the animal in deep, stage IV anesthesia [3]. Establishing animal models is an essential prerequisite of the development of new therapeutic interventions on human diseases. Monkey species provide appropriate preclinical models that can closely reflect human's physical and physiological characteristics because of their very close phylogenetic relationship to human beings [4].

3 Feature-Based Multi-Modality Registration of Retinal Images Using Adaptive Algorithm

3.1 Image Binarization via Discriminant Analysis

Prior to fusion, image pairs need to be registered pixel-by-pixel through a mapping function T. In our new registration algorithm, we firstly binarize the reference and input images. The angiogram grayscale image is the reference image, and fundus color image is the input image. The global adaptive threshold developed by Otsu [6][7] is used to convert the gray level colors to only black and white. The output binary image has values of 0 (black) for all pixels with the original luminance/intensity less than Otsu's threshold and 1 (white) for all other pixels. The threshold is a normalized intensity value that lies in the range [0, 1]. The Otsu's method chooses the optimal threshold to minimize the intra-class variance of the black and white pixels and to maximize between-class variance in a grayscale image. The algorithm calculates the statistics of the image itself to set the threshold and use the histogram to choose its value at some percentile as a reference value of the region strength. Therefore, Otsu's method is non-parametric and non-supervised. When binarizing a color image, it is converted into 8-bit gray scale prior to the binary image. 0.5236 for red, 0.1232 for green and 0.3256 for blue are the default weight parameters. In this method, we extract blue color as an example when converting to gray scale image because blue intensity histogram is the closest one to the normal distribution and the vessels on the retinal images contain stronger average blue color information than red and green or any other RGB combination.

3.2 Extract Vasculature via Canny Edge Detector

A digital curve display can be represented by an integer sequence based on the position of the current edge pixel to the eight neighbors at the 2D spatial domain: Ni {1, 2, 3, 4, 5, 6, 7, 8}, representing evenly distributed angles. The Canny Edge Detector detects the edges at zero-crossings of the second directional derivative of the image. The zero-crossings of Canny's method correspond to the first directional-derivative's maxima and minima in the direction of the gradient. Each pixel's edge gradient is computed and compared with gradients of its neighbors along the gradient direction. If the gradient at $P_{x,y}$ is greater than both the $P_{x+1,y+1}$ and $P_{x-1,y-1}$, then the $P_{x,y}$ will be identified as the maxima simply.

3.3 Control Points Selection Using Adaptive Algorithm

We select the control points at the vessel bifurcations on the Canny edge. The vessel tracking is efficiently performed in our adaptive exploratory algorithm without traveling at every pixel. We trace the vasculature by locating an initial point and exploiting the local neighbors [5]. We firstly split the entire image into two equal size bifurcation blocks of West and East. Considering retinal images, good control points always come out of the east or west side of the optic disk, rather than the north or south side. From the west block's Northwest corner, read the edge pixels from West to East and from North to South. Mark the current direction as "East" whenever the edge pixels are heading toward East, Southeast, or Northeast. Increase the step count once when the pixel is moving toward "East", while straight North or straight south does not count for steps.

If direction starts to change, i.e. change from East to West, the step count needs to be compared with ROLLBACK threshold step. If smaller, roll back the most recent change of step count; otherwise, keep the last step direction and reset the step count. The direction-changing pixel is a possible control point to be determined later. Repeat this sequence and mark the most recent possible control point as a true control point when the step count is equal to the threshold MAXSTEP and the previous step count is equal or greater than MAXSTEP as well. At the east block, read the Canny edge pixels from East to West. The rest procedures are same except the direction reading the edge pixels is from East to West, and direction change sign is from Westward to Eastward.

3.4 Control Point Pair Matching Using Shape Similarity

The 2D affine transformation model requires three pairs of control points $\{(x_i, y_i), (u_i, v_i)\}$ $(i = 1, 2, 3)$. The first element of each pair is from the reference image and the second element is from the input image. Firstly, we take the image having less number of control points as the grouping base. Suppose the image one has n control points, and the image two has m control points, and $m < n$, then m will be the group number that how many groups of control points we have. Secondly, we combine all control point in the image one with each control point in the image two, and we get m by n control point pairs totally. We now calculate the distance |d| between each control point pair within each group. Thirdly, inside each group, we choose the pair with minimum |d|. The assumption we use the distance as the measurement of the control point pair is based on the fact that two images do not have huge rotation, shearing or translation, and thus the same features on each image are close to each other. If there are two or more control points in one image matching the same control point in the other image, the true match will always have smaller |d| than the false match. Finally, we select the three smallest distance control point pairs as final (x, y) and (u, v) pairs for the transformation model.

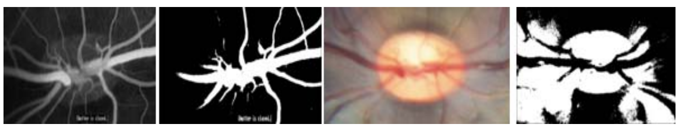

Fig. 1 Original and Binary Images (Otsu Threshold) (Left to Right: Angiogram Grayscale Image; Binary Image; Fundus Color Image; Binary Image.)

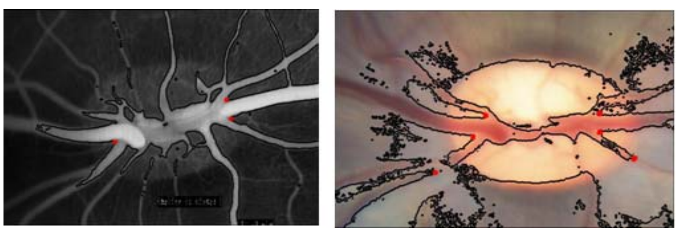

Fig. 2 (IVFA, Fundus) Image Control Point Selection

4 Optimization Fusion Based on Mutual Pixel Count Maximization

A successful fusion is one with a good superposition of retinal blood vessels. The combined image created from the control points selected in the previous registration step does not meet such criteria. An optimization procedure is needed to adjust these control points in order to achieve an optimal result. We have developed a new automated optimization iteration algorithm based on Mutual-Pixel-Count maximization. A refinement of the solution is obtained at the end of each loop, and finally a satisfying fused image is generated at the end of the iteration.

4.1 Mutual Pixel Count (MPC)

The MPC measures the retinal vasculature overlap for corresponding pixels in both images. When the vasculature pixel (black) transforms (u, v) coordinates on the input image are corresponding to a vasculature pixel's (x, y) coordinates on the reference image, the MPC is incremented by one. MPC is assumed to be maximal if the image pair is geometrically aligned by the transformation.

4.2 Global Maxima v.s. Local Maxima

To achieve optimization, global optimization scheme is desirable by achieving global maxima, but with the tradeoff on expensive computation cost. In practice, a local optimization schema is usually employed to reduce computation cost. However, local optimization can be attracted to local maxima. Thus, a new local maxima scheme is developed to achieve a global maxima equivalent result at an efficient computation cost. The entire retinal vasculature is split into three regions, i.e. west region, middle region (optic nerve head), and east region.

Only two regions out of three are selected for MPC calculation. The east region and west region are the preferred ones. The middle region is the backup in case that either of the former regions is not qualified. If the black area of the west region from the binary image is greater than a threshold, it will not be selected. By calculating partial retinal vasculature, we are able to obtain an optimal result by achieving a maximal MPC that is very close to the global maxima. If the side region reaches over a certain threshold percentage of black area, the retinal vessels cannot be well extracted among the overwhelming black pixels.

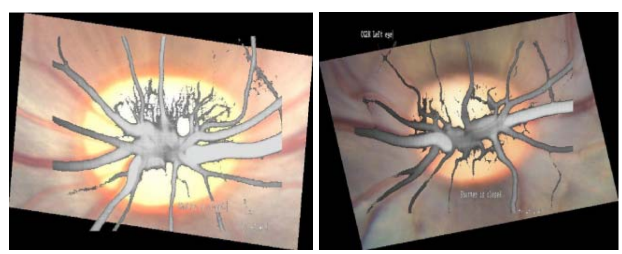

Fig. 3 Fused Images of (a) Monkey 1and (b) Monkey 2

4.3 Optimization Iteration

Our optimization algorithm finds an optimal similarity measure by refining transformation parameters in an ordered way. During the iteration, control points of the reference image are fixed and that of the input image are subject to adjustment.

Increase control point's x coordinate by a step size s initially. If the MPC is increased due to movement, keep increasing by the step size s until MPC stops increasing. Repeat this sequence for y coordinate as well. Secondly decrease control point's x coordinate and y coordinate by a step size s until MPC increasing.

Repeat this sequence for all other control points until MPC stops increasing. A maximum allowable loop number L is set to avoid redundant computation for mismatched control points, which leads to the fusion failure. Convergence criteria are used to determine when the iteration is finished.

4.4 Parameters Extraction

Once we have three pairs control points' coordinates available, we are able to apply them to the 2D affine model and solve the Gaussian matrix to get the parameters P {a1, a2, a3, a4, b1, b2}.

$$\begin{bmatrix} u_1 \\ v_1 \\ u_2 \\ v_2 \\ u_3 \\ v_3 \end{bmatrix} = \begin{bmatrix} x_1 & y_1 & 1 & 0 & 0 & 0 \\ 0 & 0 & 0 & x_1 & y_1 & 1 \\ x_2 & y_2 & 1 & 0 & 0 & 0 \\ 0 & 0 & 0 & x_2 & y_2 & 1 \\ x_3 & y_3 & 1 & 0 & 0 & 0 \\ 0 & 0 & 0 & x_3 & y_3 & 1 \end{bmatrix} \begin{bmatrix} a_1 \\ a_2 \\ b_1 \\ a_3 \\ a_4 \\ b_2 \end{bmatrix} \quad (1)$$

5 Histograms and Probability Distributions

An automatic approach for multi-modality retinal image registration has been developed using the feature-based method. Image binarization is the first step, which is to provide the input data for the Canny Edge Detector. The selected Otsu method chooses the optimal threshold to minimize the intra-class variance of the black and white pixels, and to maximize the between-class variance in the gray scale image, which is both nonparametric and unsupervised. A discrete image with N*M pixels is considered, with retinal vessels (objects) in one class and the optic disk (background) in another class. Occurrence of color component level is described as co-occurrence matrix of relative frequencies. The occurrence probability function is then estimated from its histogram, which is formulated as (2):

$$p(k)=\frac{h(k)}{\sum h(k)} \quad (2)$$

where p(k) is the probability distribution function and h(k) is the histogram function.

6 Discrete Entropy in Image Fusion

The discrete entropy is a measure of information content, which is interpreted as the average uncertainty of the information source. The discrete entropy is the summation of products of the probability of the outcome multiplied by the log of the inverse of probability of the outcome, taking into considerations of all possible outcomes {1, 2, …, n} as the color component level in the event $\{x_1, x_2, \ldots, x_n\}$, where p(i) is the probability at the gray level of i, which contains all the histogram counts. Discrete entropy H(x) is formulated as (3).

$$H(x)=\sum_{i=1}^{k} p(i)\log_2\frac{1}{p(i)} = -\sum_{i=1}^{k} p(i)\log_2 p(i) \quad (3)$$

Table 1 Entropy of Image Fusion for Monkeys 1 and 2

Global Entropy	Image A	Image B	Fusion
Monkey 1	7.3842	6.9680	6.5326
Monkey 2	6.7391	7.3238	6.1550

7 Color Component Energy

The color component energy measure indicates how the color elements are distributed. Its formulation is shown in (4), where E(x) represents each of three color component energy with 256 bins and p(i) refers to the probability distribution functions of the different color levels, which contains the histogram counts. For any constant value of the color component level, the energy measure reaches its maximum value of 1. The larger energy corresponds to lower color component level numbers and the smaller one corresponds to higher color component level numbers.

$$E(x)=\sum_{i=1}^{k} p(i)^2 \quad (4)$$

Table 2 Energy of Image Fusion for Monkeys 1 and 2

Energy	Image A	Image B	Fusion
Monkey 1	0.0076	0.0098	0.0359
Monkey 2	0.0133	0.0077	0.0713

8 Image Fusion Redundancy

The symmetric information measure can be introduced to indicate redundancy in image fusion, which reaches the minima of zero when all variables are independent. It is formulated as (5):

$$R=\frac{I(X;Y)}{H(X)+H(Y)} \quad (5)$$

where H(X) and H(Y) are entropies of two raw images and I(X, Y) is the mutual information.

$$I(X;Y)=\sum_{X,Y} p_{XY}(X,Y)\log_2 \frac{p_{XY}(X,Y)}{p_X(X)p_Y(Y)} \qquad (6)$$

where p_{XY} is the joint probability function; p_X and p_Y are the probability distributions of two raw images. For cases of Monkeys 1 and 2, redundancy between the fused image and raw images are shown in Table 3.

Table 3 Information Redundancy of Image Fusion

Information Redundancy	Fusion Image v.s. Image A	Fusion Image v.s. Image B
Monkey 1	0.0593	0.0303
Monkey 2	0.0415	0.0831

9 Conclusion

An automatic approach for the multi-modality retinal image registration has been developed using the feature-based method, which has been evaluated in both quantitative and qualitative approaches. This approach is robust to handle multi-sensor retinal image registration as long as the input image, compared with the reference image does not have significant rotation or translation. The mismatch occurs if there is a huge rotation or translation of the input image, the common feature-based approaches have the difficulty in dealing with. The solution is to implement the area-based registration method to align the image beforehand. The feature-based multi-modality registration algorithm proposed serves as the fundamental step for the hybrid area-based and feature-based systems, which can be easily applied to a wide variety of examples in some practical implementations. To investigate the whole set of complex processes quantitatively, the information theory is proposed and applied. The discrete entropy, color component energy and information redundancy have been employed as measures to evaluate image registration and image fusion.

References:

[1] F. Maes, A. Collignon, D. Vandermeulen, G. Marchal, P. Suetens, “Multimodality Image Registration by Maximization of Mutual Information”, IEEE Transactions on Medical Imaging, 1997, V 16, N2, pp. 187-198.

[2] Z. Ye, H. Cao, S. Iyengar, H. Mohamadian, "Practical Approaches on Medical and Biometric System Identification for Pattern Recognition, Data Fusion and Information Measuring", Systems Engineering Approach to Medical Automation, Chapter 6, Artech House Publishers, 2008

[3] J. Beach, J. Ning, B. Khoobehi, “Oxygen Saturation in Optic Nerve Head Structures by Hyperspectral Image Analysis”, Current Eye Research, V32, 2007, pp. 161-170

[4] Tsukuba Primate Research Center, National Institute of Biomedical Innovation Hachimandai 1-1, Tsukubashi, Ibaraki, Japan.

[5] H. Li, “Multi-Sensor Image Registration and Fusion”, PhD Dissertation, University of California, Santa Barbara, 1993

[6] N. Otsu, "A Threshold Selection Method from Gray-Level Histograms", IEEE Transactions on Systems, Man, & Cybernetics, V9, P 62-66, 1979

[7] P. Sahoo, A. Farag, Y. Yeap, “Threshold Selection Based on Histogram Modeling”, IEEE Transactions on Systems, Man and Cybernetics, V1, Oct, 1992, pp. 351 – 356

[8] J. Canny, "A Computational approach to edge detection", IEEE Transactions on Pattern Analysis and Machine Intelligence, V8, Nov, 1986, pp. 679-698

[9] W. Green, “Canny Edge Detector”, Department of Mechanical Engineering, Drexel University, Philadelphia, PA 19104, 2002

[10] G. Matsopoulos, N. Mouravliansky and K. Delibasis, “Automatic retinal image registration scheme using global optimization techniques”, IEEE Transactions on Information Technology in Biomedicine, V3, Mar, 1999, pp. 47 - 60

[11] F. Laliberte, L. Gagnon, “Registration and fusion of retinal images - An evaluation study”, IEEE Transactions on Medical Imaging, 2003, V22, N5, pp. 661-673

[12] H. Cao, “A Novel Automated Approach of Multi-modality Retinal Image Registration and Fusion”, Ph.D. Dissertation, Louisiana State University, Baton Rouge, LA, 2008

[13] Z. Ye, “Artificial Intelligence Approach for Biomedical Sample Characterization Using Raman Spectroscopy”, IEEE Transactions on Automation Science and Engineering, Volume 2, Issue 1, pp. 67-73, ITASC7, ISSN 1545-5955, January, 2005

[14] T. Cover and J. Thomas, "Elements of Information Theory", 2nd Edition, New York: Wiley, 2005

[15] D. MacKay, "Information Theory, Inference and Learning Algorithms", University of Cambridge Press, 2005